Benzothiazinones Kill Mycobacterium tuberculosis by Blocking Arabinan Synthesis

Vadim Makarov, *et al.*

Science **324**, 801 (2009);
DOI: 10.1126/science.1171583

consultant, and board member of Cellular Dynamics International (CDI). He also serves as a scientific adviser to and has financial interests in Tactics II Stem Cell Ventures. I.I.S. is a founder, stock owner, and consultant for CDI. The authors are filing a patent based on the results reported in this paper. Combination 6 and 19 episomal vectors are deposited in Addgene (Cambridge, MA), and vector-free human iPS cell subclones are deposited in the WiCell International Stem Cell (WISC) Bank (Madison, WI). Microarray data are deposited in the Gene Expression Omnibus (GEO) database (accession number GSE15148).

Supporting Online Material
www.sciencemag.org/cgi/content/full/1172482/DC1
Materials and Methods
Figs. S1 to S4
Tables S1 to S8
References

18 February 2009; accepted 17 March 2009
Published online 26 March 2009;
10.1126/science.1172482
Include this information when citing this paper.

Benzothiazinones Kill *Mycobacterium tuberculosis* by Blocking Arabinan Synthesis

Vadim Makarov,[1,2]* Giulia Manina,[1,3]* Katarina Mikusova,[1,4]* Ute Möllmann,[1,5]* Olga Ryabova,[1,2] Brigitte Saint-Joanis,[1,6] Neeraj Dhar,[7] Maria Rosalia Pasca,[1,3] Silvia Buroni,[1,3] Anna Paola Lucarelli,[1,3] Anna Milano,[1,3] Edda De Rossi,[1,3] Martina Belanova,[1,4] Adela Bobovska,[1,4] Petronela Dianiskova,[1,4] Jana Kordulakova,[1,4] Claudia Sala,[1,7] Elizabeth Fullam,[1,7] Patricia Schneider,[1,7] John D. McKinney,[7] Priscille Brodin,[8] Thierry Christophe,[8] Simon Waddell,[1,9] Philip Butcher,[1,9] Jakob Albrethsen,[1,10] Ida Rosenkrands,[1,10] Roland Brosch,[1,6] Vrinda Nandi,[1,11] Sowmya Bharath,[1,11] Sheshagiri Gaonkar,[1,11] Radha K. Shandil,[1,11] Venkataraman Balasubramanian,[1,11] Tanjore Balganesh,[1,11] Sandeep Tyagi,[12] Jacques Grosset,[12] Giovanna Riccardi,[1,3] Stewart T. Cole[1,7]†

New drugs are required to counter the tuberculosis (TB) pandemic. Here, we describe the synthesis and characterization of 1,3-benzothiazin-4-ones (BTZs), a new class of antimycobacterial agents that kill *Mycobacterium tuberculosis* in vitro, ex vivo, and in mouse models of TB. Using genetics and biochemistry, we identified the enzyme decaprenylphosphoryl-β-D-ribose 2′-epimerase as a major BTZ target. Inhibition of this enzymatic activity abolishes the formation of decaprenylphosphoryl arabinose, a key precursor that is required for the synthesis of the cell-wall arabinans, thus provoking cell lysis and bacterial death. The most advanced compound, BTZ043, is a candidate for inclusion in combination therapies for both drug-sensitive and extensively drug-resistant TB.

The loss of human lives to tuberculosis (TB) continues essentially unabated as a result of poverty, synergy with the HIV/AIDS pandemic, and the emergence of multi- drug- and extensively drug-resistant strains of *Mycobacterium tuberculosis* (*1*–*3*). Despite some recent successes, such as the discovery of the diarylquinoline drug TMC207 (*4*) and the promise of the bicyclic nitroimidazole compounds (*5*–*8*), and because of the high attrition rate in drug development (*9*), much greater effort is required to find better drugs in order to meet the desired goals of killing persistent tubercle bacilli and reducing TB treatment duration from 6 to less than 3 months (*10*, *11*).

A series of sulfur-containing heterocycles was synthesized and tested for antibacterial and antifungal activity (*12*, *13*). Among their derivatives, compounds belonging to the nitrobenzothiazinone (BTZ) class showed particular promise in terms of their potency and specificity for mycobacteria. One of them, 2-[2-methyl-1,4-dioxa-8-azaspiro[4.5]dec-8-yl]-8-nitro-6-(trifluoromethyl)-4*H*-1,3-benzothiazin-4-one (BTZ038), was selected for further studies. This compound (series number 10526038; $C_{17}H_{16}F_3N_3O_5S$, with a molecular weight of 431.4; log*P* = 2.84) (Fig. 1A) was synthesized in seven steps with a yield of 36%. Structure activity relationship work showed that the sulfur atom and the nitro group at positions 1 and 8, respectively, were critical for activity. BTZ038 has a single chiral center, and both enantiomers, BTZ043 (*S*) and BTZ044 (*R*), were found to be equipotent in vitro. Because early metabolic studies with bacteria or mice indicated that the nitro group could be reduced to an amino group, and because many TB drugs are prodrugs that require activation by *M. tuberculosis* (*14*), the *S* and *R* enantiomers of the amino derivatives and the likely hydroxylamine intermediate were synthesized and tested for antimycobacterial activity in vitro (table S1). The amino (BTZ045, *S* and *R*) and hydroxylamine (BTZ046) derivatives were substantially less active (500- to 5000-fold).

The minimal inhibitory concentrations (MICs) of a variety of BTZs against different mycobacteria were very low, ranging from ~0.1 to 80 ng/ml for fast growers and from 1 to 30 ng/ml for members of the *M. tuberculosis* complex (*13*). The MIC of BTZ043 against *M. tuberculosis* H37Rv and *Mycobacterium smegmatis* were 1 ng/ml (2.3 nM) and 4 ng/ml (9.2 nM), respectively (Table 1), which compares favorably with those of the existing TB drugs isoniazid (INH) (0.02 to 0.2 μg/ml) and ethambutol (EMB) (1 to 5 μg/ml) (*14*). From structure activity relationship studies, >30 different BTZ derivatives showed MICs of <50 ng/ml against tubercle

Table 1. MIC of BTZ043 against three different mycobacterial species and their resistant mutants.

Strain	MIC (ng/ml)	Codon	Amino acid
M. smegmatis mc^{2}155	4	TGC	Cysteine
M. smegmatis MN47	4000	GGC	Glycine
M. smegmatis MN84	>16,000	TCC	Serine
M. bovis BCG	2	TGC	Cysteine
M. bovis BCG BN2	>16,000	TCC	Serine
M. tuberculosis H37Rv	1	TGC	Cysteine
M. tuberculosis NTB9	250	GGC	Glycine
M. tuberculosis NTB1	10,000	TCC	Serine

[1]New Medicines for Tuberculosis (NM4TB) Consortium (www.nm4tb.org). [2]A. N. Bakh Institute of Biochemistry, Russian Academy of Science, 119071 Moscow, Russia. [3]Dipartimento di Genetica e Microbiologia, Università degli Studi di Pavia, via Ferrata, 1, 27100 Pavia, Italy. [4]Department of Biochemistry, Faculty of Natural Sciences, Comenius University, Mlynska dolina, 84215 Bratislava, Slovakia. [5]Department of Molecular and Applied Microbiology, Leibniz Institute for Natural Product Research and Infection Biology–Hans Knoell Institute, Beutenbergstrasse 11a, D-07745 Jena, Germany. [6]Institut Pasteur, Integrated Mycobacterial Pathogenomics, 25-28, Rue du Docteur Roux, 75724 Paris Cedex 15, France. [7]Global Health Institute, Ecole Polytechnique Fédérale de Lausanne, CH-1015 Lausanne, Switzerland. [8]Inserm Avenir Group, Institut Pasteur Korea, 39-1 Hawolgok-dong, Seongbuk-gu, 136-791 Seoul, Korea. [9]Division of Cellular and Molecular Medicine, St. George's Hospital, University of London, Cranmer Terrace, SW17 ORE London, UK. [10]Statens Serum Institut, Department of Infectious Disease Immunology, Artillerivej 5, DK-2300 Copenhagen S, Denmark. [11]AstraZeneca India, Bellary Road Hebbal, Bangalore, India. [12]Center for Tuberculosis Research, Johns Hopkins University School of Medicine, Baltimore, MD 21231, USA.

*These authors contributed equally to this work.
†To whom correspondence should be addressed. E-mail: stewart.cole@epfl.ch

bacilli (examples are shown in table S2). Crucially, BTZ043 displayed similar activity against all clinical isolates of *M. tuberculosis* that were tested, including multidrug-resistant and extensively drug-resistant strains, indicating that it targets a previously unknown biological function (table S3). BTZ043 is bactericidal, reducing viability in vitro by more than 1000-fold in under 72 hours (Fig. 1B), which is comparable to the killing effect seen with INH. In two different model systems (auxotrophy and starvation) involving metabolically inert *M. tuberculosis*, BTZ043 was less effective, which implies that it blocks a step in active metabolism, similar to INH (*14*).

Observation with time-lapse fluorescence microscopy of individual *M. smegmatis* cells [expressing green fluorescent protein (GFP)] growing in a microfluidic device (*15*) revealed that upon exposure to BTZ043, the growth rate decreased rapidly followed by a swelling of the poles and lysis of the cells after a few hours (movie S1). *M. tuberculosis* showed similar but delayed behavior (movie S2 and fig. S1).

Comparative transcriptome analysis of *M. tuberculosis* offered no evidence of mutagenic or nitrosative gene expression signatures after treatment with BTZ043, although expression of 60 genes was induced (table S4), and this was corroborated with proteomics. The transcriptional signature most resembled that generated by the cell wall inhibitors INH, isoxyl, and ethionamide, with the greatest overlap seen with the response to EMB treatment (*16*, *17*). This is consistent with cell lysis and indicated that BTZ targets cell wall biogenesis.

We then tested the uptake, intracellular killing, and potential cytotoxicity of BTZ compounds in an ex vivo model using a high-content screening approach (*18*, *19*) in order to monitor macrophages infected with *M. tuberculosis* expressing GFP. Macrophages treated with BTZ043 were protected (fig. S2) as compared with those treated with the amino derivative BTZ045 or the negative controls [dimethyl sulfoxide (DMSO)]. The deduced MIC of BTZ043 was <10 ng/ml, indicating that this compound is more potent than INH (100 ng/ml) and rifampin (>1 μg/ml) against intracellular bacteria (Fig. 1C). In contrast, the amino metabolite BTZ045 had an MIC of >1μg/ml, which is consistent with the in vitro findings (table S1). As a direct correlate of the antibacterial effect, there was extensive macrophage survival when all compounds were used at doses well above the MIC. BTZ043 was more cytotoxic than INH (Fig. 1C) at the highest concentration tested (10 μg/ml) but nonetheless has a favorable selectivity index of >100. Additional in vitro toxicology tests revealed no particularly unfavorable effects (table S4).

The in vivo efficacy of BTZ043 was assessed 4 weeks after a low-dose aerosol infection of BALB/c mice in the chronic model of TB. Four weeks of treatment with BTZ043 reduced the bacterial burden in the lungs and spleens by 1 and 2 logs, respectively, at the concentrations used (Fig. 1D). Additional results suggest that BTZ efficacy is time- rather than dose-dependent. Acute (5 g/kg) and chronic (25 and 250 mg/kg) toxicology studies in uninfected mice showed that, even at the highest dose tested, there were no adverse anatomical, behavioral, or physiological effects after one month (table S5).

To find the target for BTZ, we employed two independent genetic approaches. First, we identified cosmids bearing DNA from *M. smegmatis* that confer increased resistance on *M. smegmatis*, and we pinpointed the region responsible by subcloning. Second, we isolated and characterized mutants of *M. smegmatis*, *M. bovis* Bacille Calmette-Guérin (BCG), and *M. tuberculosis* displaying high-level BTZ resistance. The first approach revealed that the *MSMEG_6382* gene of *M. smegmatis* or its *M. tuberculosis* ortholog *rv3790* mediated increased resistance (Fig. 2A), whereas the second showed that drug-resistant mutants harbor missense mutations in the same gene (Table 1). Biochemical studies showed that *rv3790* and the neighboring gene *rv3791* code for proteins that act in concert to catalyze the epimerization of decaprenylphosphoryl ribose (DPR) to decaprenylphosphoryl arabinose (DPA) (*20*), a precursor for arabinan synthesis without which a complete mycobacterial cell wall cannot be produced. These essential membrane-associated enzymes (*20*–*23*) have been suggested to act as decaprenylphosphoryl-β-D-ribose oxidase and decaprenylphosphoryl-D-2-keto erythro pentose reductase, respectively, and we propose naming them DprE1 and DprE2. In all of the drug-resistant mutants we examined, the same

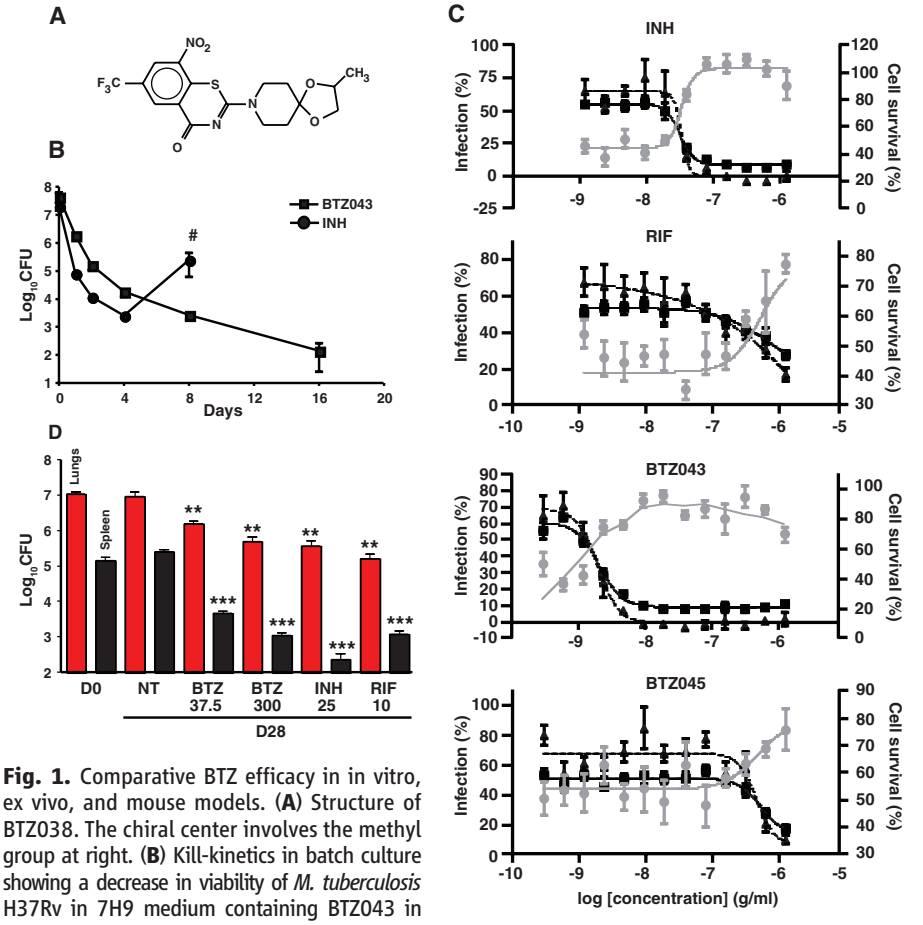

Fig. 1. Comparative BTZ efficacy in in vitro, ex vivo, and mouse models. (**A**) Structure of BTZ038. The chiral center involves the methyl group at right. (**B**) Kill-kinetics in batch culture showing a decrease in viability of *M. tuberculosis* H37Rv in 7H9 medium containing BTZ043 in comparison with INH (both at 200 ng/ml). The regrowth after treatment with INH (pound sign indicates the experiment was terminated because of resistance) is not seen with BTZ043. (**C**) Response of macrophages infected with GFP-labeled *M. tuberculosis* to treatment with different compounds, expressed in percent of bacterial load (triangles), cell survival (circles), and infected cells (squares) relative to compound concentration in grams per milliliter. Each percentage is based on DMSO and INH controls from the same experiments. For each concentration, the mean ± SEM of the quadruplicate are reported. For the original images, see fig. S2. (**D**) Efficacy of BTZ043 in a mouse model of chronic tuberculosis compared with INH, rifampin (RIF), and untreated controls. Red and black columns correspond to the bacterial load in the lungs and spleens, respectively, of chronically infected BALB/c mice (4 weeks after infection) at day 0 (D0), before treatment. The remaining columns show bacterial loads at day 28 in untreated animals (NT) (5 per group) or in mice treated with various drugs at the doses indicated (milligrams per kilogram of body weight per day). Bars represent the mean ± SEM; data are representative of two independent experiments from two different centers. $^{**}P = 0.001$; $^{***}P < 0.000001$.

codon of *rv3790* (*dprE1*) was affected, in which Cys387 was replaced by Ser or Gly codons, respectively (Table 1). Mutants, harboring alleles such as those in MN47 or MN84, were rare, arising at a frequency of $<10^{-8}$, and were dominant over the wild-type gene upon introduction into a BTZ-susceptible mycobacterium. Comparative genomics revealed that the BTZ resistance–determining region of *rv3790* was highly conserved in orthologous genes from various actinobacteria, except that in a few cases Cys387 was replaced by Ser or Ala (Fig. 2B). The corresponding bacteria, *M. avium* and *M. aurum*, were found to be naturally resistant to BTZ (table S3), thus supporting the identification of DprE1/Rv3790 as the target.

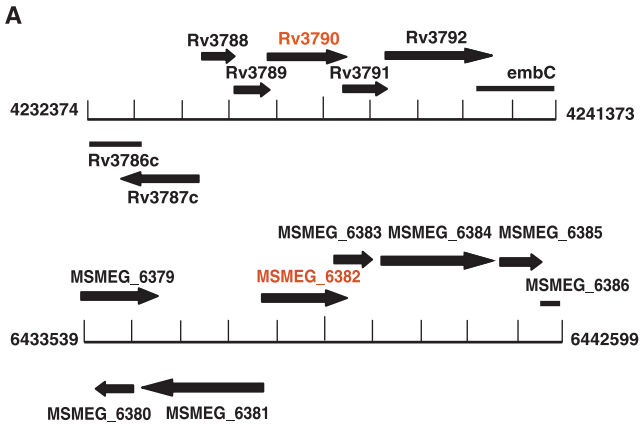

B

```
                                361                 381                 401                 420
                                 |                   |                   |                   |
M. tuberculosis (Rv3790)        SFLNVFKLFGPRNQAPLSFPIPGWNICVDFPIKDGLGKFVSELDRRVLEFGGRLYTAKDS
M. bovis                        SFLNVFKLFGPRNQAPLSFPIPGWNICVDFPIKDGLGKFVSELDRRVLEFGGRLYTAKDS
M. leprae                       SFLNVFKLFGPGNQAPLSFPIPGWNICVDFPIKSGLNEFVNKLDRRVMELGGRLYTAKDS
M. avium                        SALNVFKLFGPGNRAPLSFPMAGWNVAMDFPNKPGVNEFLNELDRRVLQFGGRVYTAKDS
M. avium paratuberculosis       SALNVFKLFGPGNRAPLSFPMAGWNVAMDFPNKPGVNEFLNELDRRVLQFGGRVYTAKDS
M. smegmatis                    SFLNVFKLFGPGNQAPLSFPIPGWNVCVDFPIKAGLHEFVTELDRRVLEFGGRLYTAKDS
M. aurum                        SFLNVFKLFGPRNQAPLSFPIPGWNISVDFPIKDGLGKFVSELDRRVLEFGGRLYTAKDS
M. gilvum                       SFLNVFKLFGPGNQAPLSFPIPGWNVCVDFPITAGLNEFLNGLDKRVLQFGGRLYTAKDS
M. vanbalenii                   SFLNVFKLFGPGNDAPLSFPIPGWNVCVDFQINPGLNEFLNGLDKRVLEFGGRLYTAKDS
M. marinum                      SFLNVFKLFGAGNQAPLSFPIPGWNICVDFPIKAGLNEFVSELDRRVMEFGGRLYTAKDS
Rhodococcus spp.                SFLNVFKLFGEGNQAPLSFPIPGWNICVDFRIKPGLNEFVTELDKRVLKFGGRLYTAKDS
Nocardia farcinica              SFLNVFKYFGQGNQAPLSFPMPGWNVCLDFPIKPGLNEFVTELDSRVLEFGGRLYTGKDS
Corynebacterium glutamicum      SALNVFKLFGEGNKAPLSYPMPGWNVCVDFPIKPGLGAFLDDLDKRVMEFGGRLYLAKES
                                * ***** **  * ****:*:.***:.:*:    *:  *:  ** **:::***:* .*:*
```

Fig. 2. Identification of the BTZ target. (**A**) Organization of genomic regions of *M. tuberculosis* and *M. smegmatis* associated with BTZ resistance. (**B**) Multiple alignment of the BTZ resistance–determining region in orthologs of Rv3790 from various actinobacteria.

Further corroboration was obtained biochemically (Fig. 3) by using membrane preparations from *M. smegmatis* to catalyze the epimerization reaction from radiolabeled DPR precursor, which was produced in situ from 5-phosphoribose diphosphate (*20*), in the presence or absence of BTZ. Addition of BTZ038, or its enantiomers BTZ043 and BTZ044, abolished the production of DPA from DPR. This reaction was scarcely affected by either the *S* or *R* forms of BTZ045 (Fig. 3A) or by BTZ046 (fig. S3). Using recombinant proteins, we found that the reaction requires both DprE1 and E2 (Rv3790 and Rv3791) (Fig. 3B), with neither enzyme alone capable of catalyzing DPA formation. Furthermore, when BN2, the highly BTZ-resistant mutant of *M. bovis* BCG, or *M. smegmatis* MN47 and MN84, with missense mutations in *MSMEG_6382* (*dprE1*) (Table 1), were used as sources of enzymes, epimerization was no longer subject to inhibition (Fig. 3C and fig. S3), thereby confirming identification of the BTZ target.

The point of BTZ inhibition in the biosynthetic pathway for arabinan precursors is shown in fig. S4, and as predicted by the gene expression profiling results, BTZ and EMB both target the same pathway, which is restricted to certain actinobacteria. The latter drug acts downstream on the EmbCAB arabinosyl transferases that use DPA, the sole arabinan donor in mycobacteria, to produce arabinogalactan or lipoarabinomannan (*24*, *25*). Consistent with DPA limitation, BTZ treatment also blocks the production of both of these species (fig. S3). Arabinogalactan plays a critical function in the mycobacterial cell envelope by acting as a covalent linker between peptidoglycan on the inside and the mycolic acids at the outer surface, thus playing a pivotal role in cellular integrity. A major difference between the two drugs lies in the potency of BTZ, which is 1000-fold more active than EMB against *M. tuberculosis*.

In conclusion, BTZ is a candidate for development into a sterilizing TB drug acting on the enzyme decaprenylphosphoryl-β-D-ribose 2′-epimerase. This target has been chemically validated in vivo and can now be used in screening for the identification of additional inhibitors.

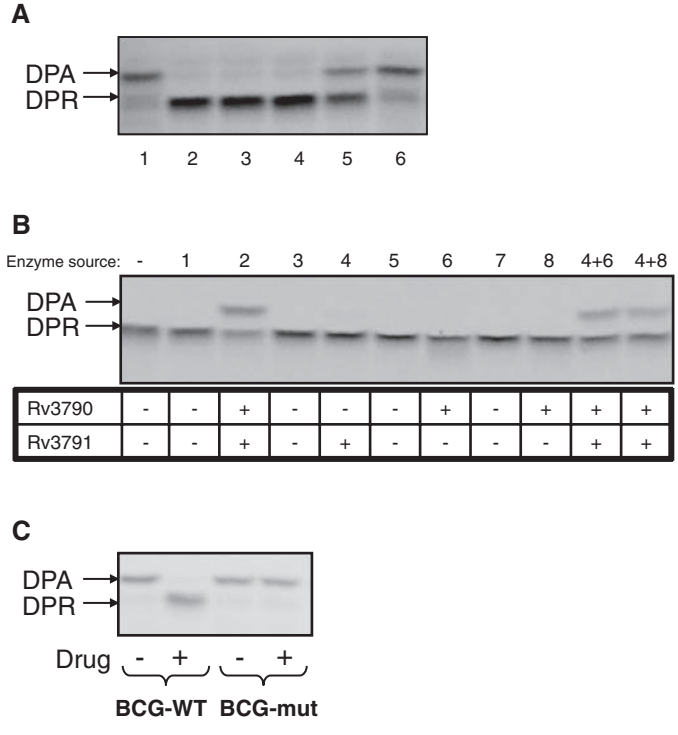

Fig. 3. Inhibition of decaprenylphosphoryl-β-D-ribose epimerization by BTZ. (**A**) Effect of different BTZ derivatives (table S1) on DPA production from DPR by using mycobacterial membranes in vitro. Lane 1, no drug control; lane 2, BTZ038; lane 3, BTZ043; lane 4, BTZ044; lane 5, BTZ045S; lane 6, BTZ045R. (**B**) Production of DPA from DPR requires both Rv3790 (DprE1) and Rv3791 (DprE2). *E. coli* strains that were used in the experiment (*26*) expressed the following *M. tuberculosis* proteins: lane 1, none; lane 2, Rv3790-Rv3791; lane 3, none; lane 4, Rv3791; lane 5, none; lane 6, Rv3790; lane 7, none; lane 8, Rv3790. (**C**) Effect of BTZ043 on DPA production by using cell wall fractions from BTZ-sensitive *M. bovis* BCG and its BTZ-resistant mutant, BN2 (Table 1).

References and Notes

1. C. Dye, *Lancet* **367**, 938 (2006).
2. N. R. Gandhi *et al.*, *Lancet* **368**, 1575 (2006).
3. M. Zignol *et al.*, *J. Infect. Dis.* **194**, 479 (2006).
4. K. Andries *et al.*, *Science* **307**, 223 (2005).
5. C. K. Stover *et al.*, *Nature* **405**, 962 (2000).

6. U. H. Manjunatha *et al.*, *Proc. Natl. Acad. Sci. U.S.A.* **103**, 431 (2006).
7. M. Matsumoto *et al.*, *PLoS Med.* **3**, e466 (2006).
8. R. Singh *et al.*, *Science* **322**, 1392 (2008).
9. T. S. Balganesh, P. M. Alzari, S. T. Cole, *Trends Pharmacol. Sci.* **29**, 576 (2008).
10. Global Alliance for TB, *Tuberculosis (Edinb.)* **81**, (suppl. 1), 1 (2001).
11. D. B. Young, M. D. Perkins, K. Duncan, C. E. Barry 3rd, *J. Clin. Invest.* **118**, 1255 (2008).
12. V. Makarov, U. Möllmann, S. T. Cole, Eurasian Patent Application EP2029583 (2007).
13. V. Makarov *et al.*, *J. Antimicrob. Chemother.* **57**, 1134 (2006).
14. Y. Zhang, C. Vilcheze, W. R. Jacobs Jr., in *Tuberculosis and the Tubercle Bacillus*, S. T. Cole, K. D. Eisenach, D. N. McMurray, W. R. Jacobs Jr., Eds. (American Society for Microbiology Press, Washington, DC, 2005), pp. 115–140.
15. N. Q. Balaban, J. Merrin, R. Chait, L. Kowalik, S. Leibler, *Science* **305**, 1622 (2004).
16. H. I. Boshoff *et al.*, *J. Biol. Chem.* **279**, 40174 (2004).
17. S. J. Waddell, P. D. Butcher, *Curr. Mol. Med.* **7**, 287 (2007).
18. V. C. Abraham, D. L. Taylor, J. R. Haskins, *Trends Biotechnol.* **22**, 15 (2004).
19. D. Fenistein, B. Lenseigne, T. Christophe, P. Brodin, A. Genovesio, *Cytometry A* **73**, 958 (2008).
20. K. Mikusova *et al.*, *J. Bacteriol.* **187**, 8020 (2005).
21. C. M. Sassetti, D. H. Boyd, E. J. Rubin, *Proc. Natl. Acad. Sci. U.S.A.* **98**, 12712 (2001).
22. B. A. Wolucka, *FEBS J.* **275**, 2691 (2008).
23. C. E. Barry, D. C. Crick, M. R. McNeil, *Infect. Disord. Drug Targets* **7**, 1 (2007).
24. K. Mikusova, R. A. Slayden, G. S. Besra, P. J. Brennan, *Antimicrob. Agents Chemother.* **39**, 2484 (1995).
25. L. J. Alderwick *et al.*, *J. Biol. Chem.* **280**, 32362 (2005).
26. Materials and methods are available as supporting material on *Science* Online.

27. We thank A. Deshpande, I. Heinemann, P. Højrup, K. Johnsson, M. K. N. Kumar, N. Kumar, L. Pagani, P. Marone, M. R. McNeil, I. Old, J. Reddy, S. Schmitt, P. Vachaspati, and C. Weigel for their help and support. Patents related to this work have been filed (WO/2007/134625, WO/2009/010163, and PCT/EP2008/001088). The NM4TB Consortium is funded by the European Commission (LHSP-CT-2005-018923), and microarray work at St George's Hospital, University of London, is supported by the Wellcome Trust (grant 062511). Microarray data are Minimum Information About a Microarray Experiment (MIAME)–compliant and deposited under accession number E-BUGS-80 at http://bugs.sgul.ac.uk/E-BUGS-80.

Supporting Online Material

www.sciencemag.org/cgi/content/full/1171583/DC1
Materials and Methods
Figs. S1 to S4
Tables S1 to S6
References
Movies S1 and S2

29 January 2009; accepted 13 March 2009
Published online 19 March 2009;
10.1126/science.1171583
Include this information when citing this paper.

Mammalian Expression of Infrared Fluorescent Proteins Engineered from a Bacterial Phytochrome

Xiaokun Shu,[1,2] Antoine Royant,[3] Michael Z. Lin,[2] Todd A. Aguilera,[2] Varda Lev-Ram,[2] Paul A. Steinbach,[1,2] Roger Y. Tsien[1,2,4]*

Visibly fluorescent proteins (FPs) from jellyfish and corals have revolutionized many areas of molecular and cell biology, but the use of FPs in intact animals, such as mice, has been handicapped by poor penetration of excitation light. We now show that a bacteriophytochrome from *Deinococcus radiodurans*, incorporating biliverdin as the chromophore, can be engineered into monomeric, infrared-fluorescent proteins (IFPs), with excitation and emission maxima of 684 and 708 nm, respectively; extinction coefficient >90,000 M^{-1} cm^{-1}; and quantum yield of 0.07. IFPs express well in mammalian cells and mice and spontaneously incorporate biliverdin, which is ubiquitous as the initial intermediate in heme catabolism but has negligible fluorescence by itself. Because their wavelengths penetrate tissue well, IFPs are suitable for whole-body imaging. The IFPs developed here provide a scaffold for further engineering.

In vivo optical imaging of deep tissues in animals is most feasible between 650 and 900 nm because such wavelengths minimize the absorbance by hemoglobin, water, and lipids, as well as light-scattering (*1*, *2*). Thus, genetically encoded IFPs would be particularly valuable for whole-body imaging in cancer and stem cell biology (*3*, *4*), gene therapy, and so on. However, excitation and emission maxima of FPs have not yet exceeded 598 and 655 nm, respectively (*5*–*7*). Somewhat longer wavelengths (644-nm excitation, 672-nm emission) have been observed in a phytochrome-based FP that incorporates phycocyanobilin (PCB) as the chromophore (*8*). However, neither incorporation of exogenous PCB nor transfer of its biosynthetic pathway into animal cells has yet been demonstrated. Bacterial phytochromes are more promising because they incorporate biliverdin IXα (BV) instead of PCB (*9*), and BV is the initial intermediate in heme catabolism by heme oxygenase (HO-1) in all aerobic organisms, including animals. For example, normal adult humans endogenously generate and metabolize 300 to 500 mg BV each day simply from routine heme breakdown (*10*). Recently, a full-length bacteriophytochrome (DrBphP) from *Deinococcus radiodurans* with a single mutation (D207H) (*11*) was reported to be red fluorescent at 622 nm upon excitation of the Soret band near 416 nm (*12*). Excitation of the Q band absorbing at 699 nm gave no fluorescence (*12*), which contradicted Kasha's rule that fluorescence occurs from the lowest excited state. Emission peaks at 710 to 725 nm have been observed from various forms of *Rhodopseudomonas palustris* (*13*) and *Pseudomonas aeruginosa* (*14*) bacteriophytochromes expressed in *Escherichia coli*, but fluorescence efficiencies have not been quantified, and reconstitution in nonbacterial systems has not yet been demonstrated.

To minimize the probability of nonradiative decay, we chose to limit DrBphP to its chromophore-binding domain (CBD), consisting of the PAS and GAF domains, which are

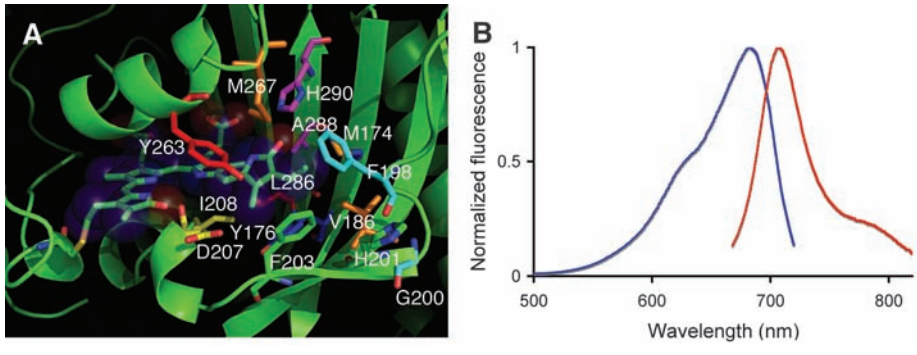

Fig. 1. Infrared fluorescent proteins created by structure-based engineering of a bacteriophytochrome. (**A**) Fourteen residues surrounding the biliverdin in DrCBD [Protein Data Bank (PDB) ID: 1ztu] (*16*) were divided into seven groups (shown in different colors) and targeted for mutagenesis. (**B**) Normalized excitation (blue) and emission (red) spectra of IFP1.4.

[1]Howard Hughes Medical Institute, University of California at San Diego, 9500 Gilman Drive, La Jolla, CA 92093–0647, USA. [2]Department of Pharmacology, University of California at San Diego, 9500 Gilman Drive, La Jolla, CA 92093–0647, USA. [3]Institut de Biologie Structurale 41, rue Jules Horowitz, 38027 Grenoble CEDEX 1, France. [4]Departments of Chemistry and Biochemistry, University of California at San Diego, 9500 Gilman Drive, La Jolla, CA 92093–0647, USA.

*To whom correspondence should be addressed. E-mail: rtsien@ucsd.edu